J|A|C|S
ARTICLES
Published on Web 04/01/2004

Electron Self-Exchange Kinetics Determined by MARY Spectroscopy: Theory and Experiment

M. Justinek,[†] G. Grampp,[†] S. Landgraf,*[,†] P. J. Hore,[‡] and N. N. Lukzen[§]

Contribution from the Institute of Physical and Theoretical Chemistry, Graz University of Technology, Technikerstrasse 4/I, A-8010 Graz, Austria; Physical and Theoretical Chemistry Laboratory, Oxford University, South Parks Road, Oxford OX1 3QZ, UK; and International Tomography Center, Institutskaya 3a, Novosibirsk 630090, Russia

Received November 7, 2003; E-mail: landgraf@ptc.tu-graz.ac.at

Abstract: The electron self-exchange between a neutral molecule and its charged radical, which is part of a spin-correlated radical ion pair, gives rise to line width effects in the fluorescence-detected MARY (magnetic field effect on reaction yield) spectrum similar to those observed in EPR spectroscopy. An increasing self-exchange rate (i.e., a higher concentration of the neutral molecule) leads to broadening and subsequent narrowing of the spectrum. Along with a series of MARY spectra recorded for several systems (the fluorophores pyrene, pyrene-d_{10} and *N*-methylcarbazole in combination with 1,2- and 1,4-dicyanobenzene) in various solvents, a theoretical model is developed that describes the spin evolution and the diffusive recombination of the radical pair under the influence of the external magnetic field and electron self-exchange, thereby allowing the simulation of MARY spectra of the systems investigated experimentally. The spin evolution of the radicals in the pair is calculated separately using spin correlation tensors, thereby allowing rigorous quantum mechanical calculations for real spin systems. It is shown that the combination of these simulations with high resolution, low noise experimental spectra makes the MARY technique a novel, quantitative method for the determination of self-exchange rate constants. In comparison to a simple analytical formula which estimates the self-exchange rate constant from the slope of the linear part of a line width vs concentration plot, the simulation method yields more reliable and accurate results. The correctness of the results obtained by the MARY method is proved by a comparison with corresponding data from the well-established EPR line broadening technique. With its less stringent restrictions on radical lifetime and stability, the MARY technique provides an alternative to the classical EPR method, in particular for systems involving short-lived and unstable radicals.

1. Introduction

The investigation of the kinetics of electron self-exchange reactions (or degenerate electron exchange) provides a useful strategy to study activated electron transfer in the framework of widely used theories (transition state theory, Marcus theory).[1] The transfer of an electron between a neutral molecule and its charged radical anion or cation occurring with the bimolecular rate constant k_{ex} according to the scheme

$$Q^{\bullet}\pm + Q \overset{k_{ex}}{\rightleftharpoons} Q + Q^{\bullet}\pm \qquad (1)$$

constitutes one of the simplest examples of an electron transfer reaction, since the related change in free energy is zero ($\Delta G^{\circ} = 0$). Consequently, in its simplest form, the Marcus reorganization energy of a self-exchange reaction is directly given by the free energy of activation, i.e., $\lambda/4 = \Delta G^{*}$. Thus, the theoretical interpretation of such reactions is significantly facilitated as compared to "ordinary" electron transfer reactions with $\Delta G^{\circ} \neq 0$, making electron self-exchange a useful model reaction for the study of topics such as activation parameters or dynamical solvent effects on rate constants.[2] In addition, the knowledge of self-exchange rate constants allows one to predict the rate constants of mixed redox reactions by using the Marcus cross relation.[3,4]

The most widely used technique to investigate homogeneous electron self-exchange kinetics for organic systems is EPR (electron paramagnetic resonance) spectroscopy.[4−10] With increasing electron self-exchange rate ν_{ex}, i.e., decreasing nuclear spin configuration lifetime τ, the EPR lines broaden (slow exchange limit) until they merge into a single line which is

[†] Graz University of Technology.
[‡] Oxford University.
[§] International Tomography Center.

(1) Bolton, J. R.; Archer, M. D. In *Electron Transfer in Inorganic, Organic and Biological Systems*; Bolton, J. R., Mataga, N., McLendon, G., Eds.; Number 228 in Advances in Chemistry; American Chemical Society: Washington, 1991; Chapter 2, p 7.
(2) Weaver, M. J. *Chem. Rev.* **1992**, *92*, 463.
(3) Marcus, R. A. *Angew. Chem., Int. Ed. Engl.* **1993**, *32*, 1111.
(4) Grampp, G. *Spectrochim. Acta A* **1998**, *54*, 2349.
(5) Eberson, L. *Adv. Phys. Org. Chem.* **1982**, *18*, 79.
(6) Grampp, G.; Jaenicke, W. *Ber. Bunsen-Ges. Phys. Chem.* **1984**, *88*, 325.
(7) Grampp, G.; Jaenicke, W. *Ber. Bunsen-Ges. Phys. Chem.* **1991**, *95*, 904.
(8) Larsen, H.; Pedersen, S. U.; Pedersen, J. A.; Lund, H. *J. Electroanal. Chem.* **1992**, *331*, 971.
(9) Jürgen, D.; Pedersen, S. U.; Pedersen, J. A.; Lund, H. *Acta Chem. Scand.* **1997**, *51*, 767.
(10) Grampp, G.; Landgraf, S.; Rasmussen, K. *J. Chem. Soc., Perkin Trans. 2* **1999**, 1897.

finally narrowed upon further increase of ν_{ex} (fast exchange limit). The electron self-exchange rate ν_{ex} is related to the concentration of the neutral molecule [Q] via the rate constant k_{ex} according to

$$\nu_{ex} = \frac{1}{\tau} = k_{ex}[Q] \tag{2}$$

The self-exchange rate constant can thus be determined from the dependence of the EPR line widths on the concentration of neutral molecule.

As in the classical EPR case, the process of electron self-exchange manifests itself in a broad range of radical or radical pair (RP) reactions,[11−18] some of which show a magnetic field effect (MFE). One important experimental method to monitor the MFE is MARY (magnetic field effect on reaction yield) spectroscopy. The MARY spectrum may be obtained by recording the emission intensity of a fluorescing singlet RP recombination product while sweeping an external magnetic field. In this case, in contrast to EPR where the electron hops between a molecule and a free radical, the self-exchange occurs between a radical which is part of a spin-correlated radical pair and its diamagnetic parent molecule according to either of the reactions

$$^{1,3}[D^{\bullet+}A^{\bullet-}] + D \overset{k_{ex}}{\rightleftharpoons} D + {}^{1,3}[A^{\bullet-}D^{\bullet+}]$$
$$^{1,3}[A^{\bullet-}D^{\bullet+}] + A \overset{k_{ex}}{\rightleftharpoons} A + {}^{1,3}[D^{\bullet+}A^{\bullet-}] \tag{3}$$

In analogy to EPR, the line width of the MARY spectrum shows an initial linear increase (broadening of the MARY line), followed by a maximum and a subsequent decrease (line narrowing) when going from low to high donor (or, analogously, acceptor) concentrations while keeping the concentration of the other RP partner constant at a low value. In the limit of slow exchange, an approximate analytical expression describing the linear increase in the line width was suggested by Weller and co-workers.[14] It is based on lifetime uncertainty broadening of RP spin levels caused by the exchange process and provides a method to estimate the self-exchange rate constant k_{ex} from the initial slope of a line width vs concentration plot.[20−22]

There appears to be no universal theory for the quantitative description of the line width effects caused by electron self-exchange in MARY spectroscopy. In this paper a theoretical model is presented which allows the ab initio calculation of MARY spectra of the systems investigated experimentally, taking into account electron self-exchange over the whole range of exchange rates. (Here the term ab initio is used in the sense of spin dynamical rather than quantum chemical calculations.) These simulations not only help to establish a deeper understanding of the mechanistic aspects of electron self-exchange reactions involving radical pairs but also provide a method to determine the rate constant k_{ex} which is more reliable and more consistent than the initial slope method mentioned above. The development of the theory and its application to experimental results obtained for the binary systems pyrene, pyrene-d_{10}, or *N*-methylcarbazole in combination with 1,2- or 1,4-dicyanobenzene in various solvents are treated in the following sections.

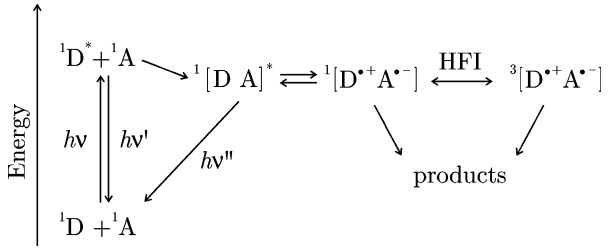

Figure 1. MARY process, involving photoinduced electron transfer and magnetic-field-dependent exciplex fluorescence. Asterisks denote electronically excited states, and the superscripts label spin multiplicities. Recombination products other than the exciplex are of minor interest and are not specified in the scheme.

2. Experimental Section

The reaction scheme of magnetic-field-affected luminescence as the basis of MARY spectroscopy[20−22] is shown in Figure 1. Upon electronic excitation of a donor (D) (or acceptor (A)) molecule by UV light, an exciplex between donor and acceptor is formed. The exciplex may either emit a fluorescence photon $h\nu''$ of lower energy than the donor fluorescence $h\nu'$ or reversibly separate into radical ions forming a spin-correlated radical ion pair (RIP) in the singlet state. Magnetic interaction of the unpaired electrons with the coupled magnetic nuclei of the RIP (hyperfine interaction, HFI) causes coherent spin evolution in the RIP which is affected by an applied magnetic field via the electron Zeeman interaction. Thus, magnetic-field-dependent singlet and triplet populations of the RIP are established. If in its S state, the RIP may undergo recombination to the exciplex, giving rise to a delayed, magnetic-field-dependent fluorescence component.

The MARY spectrometer used is based on the design described by McLauchlan, Steiner, and co-workers[19] and is described in detail in ref 20. Continuous light excitation of the sample is performed at a wavelength depending on the fluorophore (320 nm for pyrene and 332 nm for *N*-methylcarbazole). While sweeping an external magnetic field (from −10 to 12 mT), exciplex fluorescence is recorded at $\lambda > 470$ nm for the pyrene systems and $\lambda > 420$ nm for the *N*-methylcarbazole systems. Field modulation at a small amplitude B_{mod} (0.2 to 1.0mT at a frequency of 225 Hz) and phase sensitive detection result in an improved signal-to-noise (*S*/*N*) ratio. The modulation technique leads to the first derivative MARY spectrum dI_B/dB versus magnetic field *B*. The field scan rate used is 3.0 mT/min; hence the duration of a single scan is about 7 min.

The peak-to-peak line width $2B_p$ is determined by fitting a first derivative Lorentz function to the experimental spectrum using a nonlinear least-squares procedure. The use of a simple Lorentz function is justified even for experimental spectra that show a low-field feature, since in all cases the fit with respect to the line shape of the main peak, and hence the value of B_p, yields satisfactory and reproducible results. When compared to more complex fitting functions, the simple Lorentz function has the advantage of yielding B_p-values that are

(11) Saik, V. O.; Lukzen, N. N.; Grigoryants, V. M.; Anisimov, O. A.; Doktorov, A. B.; Molin, Y. N. *Chem. Phys.* **1984**, *84*, 421.
(12) Werst, D. W. *Chem. Phys. Lett.* **1993**, *202*, 101.
(13) Werst, D. W. *Chem. Phys. Lett.* **1996**, *251*, 315.
(14) Staerk, H.; Treichel, R.; Weller, A. *Chem. Phys. Lett.* **1983**, *96*, 28.
(15) Batchelor, S. N.; Kay, C. W. M.; McLauchlan, K. A.; Shkrob, I. A. *J. Phys. Chem.* **1993**, *97*, 13250.
(16) Krüger, H. W.; Michel-Beyerle, M. E.; Seidlitz, H. *Chem. Phys. Lett.* **1982**, *87*, 79.
(17) Krüger, H. W.; Michel-Beyerle, M. E.; Knapp, E. W. *Chem. Phys.* **1983**, *74*, 205.
(18) Grigoryants, V. M.; McGrane, S. D.; Lipsky, S. *J. Chem. Phys.* **1998**, *109*, 7354.
(19) Hamilton, C. A.; Hewitt, J. P.; McLauchlan, K. A.; Steiner, U. E. *Mol. Phys.* **1988**, *65*, 423.
(20) Grampp, G.; Justinek, M.; Landgraf, S. *Mol. Phys.* **2002**, *100*, 1063.
(21) Grampp, G.; Justinek, M.; Landgraf, S. *RIKEN Rev.* **2002**, *44*, 82.
(22) Justinek, M.; Grampp, G.; Landgraf, S. *Phys. Chem. Chem. Phys.* **2002**, *4*, 5550.

relatively insensitive to the modulation amplitude B_{mod}.[23] All experimental B_p values given in this work are obtained by averaging the B_p-values yielded by the Lorentz fits of a number of individual experimental spectra. Depending on their *S*/*N* ratio, between three and six spectra are recorded for the averaging, yielding B_p-values with a standard deviation of 2 to 6%.

MARY spectra are recorded for varying concentrations of one reaction component while the concentration of the other component is kept at a constant value which is chosen as low as possible yet high enough to allow for a sufficient *S*/*N* ratio. For the *N*-methylcarbazole/dicyanobenzene (MCBZ/DCB) couples, both the donor and acceptor concentrations are varied separately, whereas, in the case of the pyrene/DCB systems, only the DCB concentration is varied due to experimental limitations such as pyrene excimer formation.[20,22] Concentrations are in the range from 1.0×10^{-4} M up to 0.30 M, depending on the *S*/*N* ratio of the system. The constant concentrations are 1.0×10^{-4} M for pyrene, 1.0×10^{-3} M for MCBZ, and 0.1 or 0.2 M for the two DCB isomers. The samples are deoxygenated by purging with argon prior to measurement. Due to the high sensitivity of the apparatus, no flow technique is necessary. The stability of the sample has been checked carefully for each system separately. Even after 10 scans, no change in the MARY spectra due to possible sample degradation is observed. All measurements are performed at 293 ± 1 K.

Pyrene (Fluka, 99%) was purified by vacuum sublimation, while pyrene-d_{10} (Aldrich, 98%) was used as received. *N*-Methylcarbazole (Aldrich, 99%) was recrystallized from ethanol, while 1,2- and 1,4-DCB (Aldrich, 98%) were recrystallized from toluene. The solvents tetrahydrofuran (THF), 1,2-dimethoxyethane (DME), methanol (MeOH), propylenecarbonate (PC), benzonitrile (BN), and *N*,*N*-dimethylformamide (DMF) were of HPLC quality and were freshly distilled after dynamic drying over molecular sieves (3 Å).

3. Theory

3.1. Basics. The MARY spectrum is usually represented by plotting the difference between the relative fluorescence intensities in the presence and absence of the magnetic field versus the magnetic field, as shown in Figure 2 a. Since the fluorescence intensity I is proportional to the product yield ϕ of the luminescent species, the relaion

$$\frac{\phi_B - \phi_0}{\phi_0} = \frac{I_B - I_0}{I_0} = \frac{I_B}{I_0} - 1 \qquad (4)$$

applies, the subscript 0 meaning $B = 0$. The spectrum always shows mirror symmetry about zero field. A common characteristic of all MARY spectra based on delayed exciplex fluorescence is an initial increase in intensity which is followed by a saturation behavior. This is a consequence of the Zeeman splitting which gradually shuts down $S-T_{\pm}$ transitions with increasing magnetic field.[19] In view of the reaction scheme given in Figure 1, less efficient S−T mixing leads to an increase in delayed exciplex fluorescence intensity. At magnetic field strengths beyond the point of saturation of the MFE, no $S-T_{\pm}$ transitions take place any more while the efficiency of the magnetic field-independent $S-T_0$ transitions remains constant over the whole field range which explains the saturation behavior. In some particular cases, a low-field feature around zero magnetic field of opposite sense with respect to the "normal" MFE can be observed, as shown in Figure 2. This low-field effect (LFE) is based on a characteristic magnetic field dependence of the HFI mechanism of S−T transitions.[24,25] It

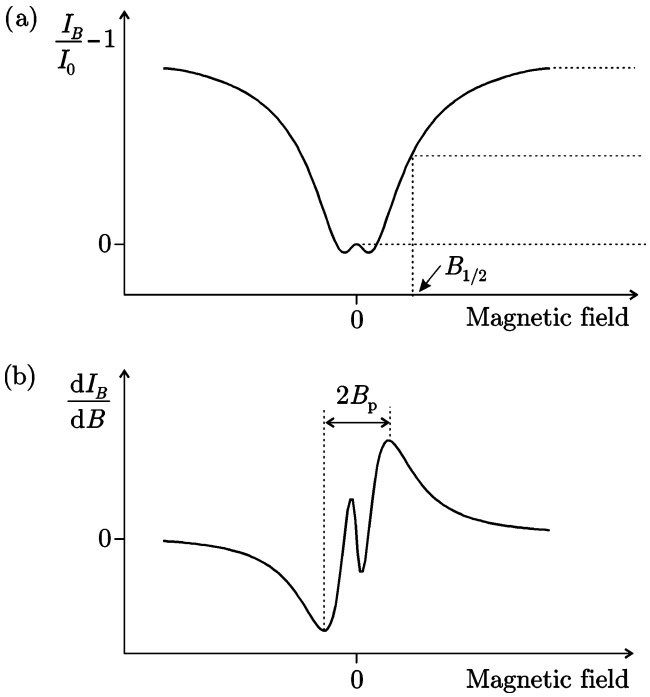

Figure 2. Schematic representation of a MARY spectrum (a) and its first derivative (b) with the characteristic parameters $B_{1/2}$, the field strength at half the saturation value of the MFE, and $B_{1/2}$, the magnetic field at the peak of the first derivative spectrum.

may be explained by differences in the conservation laws of spin angular momentum in zero and weak magnetic field.[24]

For the systems studied in this work, the size of the MFE at the saturation value is as small as 0.2 to 2%. To allow the observation of such small effects with a good *S*/*N* ratio, a modulation technique with phase-sensitive detection of exciplex fluorescence is applied, yielding the first derivative of the unmodulated MARY spectrum with respect to the magnetic field B; see Figure 2b.

Parameters used for the quantitative description of a MARY spectrum are $B_{1/2}$, the magnetic field strength at which half the saturation value of the MFE is reached, and the peak position B_p of the modulated MARY spectrum which corresponds to the point of inflection in the unmodulated spectrum. If one assumes an approximate Lorentzian line shape of the MARY spectrum, which implies neglecting the low-field feature, B_p is related to $B_{1/2}$ via

$$B_{1/2} = \sqrt{3} B_p \qquad (5)$$

The line width and thus $B_{1/2}$ are determined mainly by the hyperfine coupling constants of the nuclei present in the RP. One useful way to express the HFI in a radical is to define an average nuclear hyperfine field B_k in a quasi-classical fashion by the root-mean-square value[26]

$$B_k = \sqrt{\sum_i a_{ik}^2 I_{ik}(I_{ik} + 1)} \qquad (6)$$

where a_{ik} and I_{ik} are, respectively, the individual isotropic HF coupling constants and nuclear spin quantum numbers in radical

(23) Justinek, M. Unpublished work.
(24) Brocklehurst, B.; McLauchlan, K. A. *Int. J. Radiat. Biol.* **1996**, *69*, 3.
(25) Stass, D. V.; Lukzen, N. N.; Tadjikov, B. M.; Molin, Y. N. *Chem. Phys. Lett.* **1995**, *233*, 444.
(26) Weller, A.; Nolting, F.; Staerk, H. *Chem. Phys. Lett.* **1983**, *96*, 24.

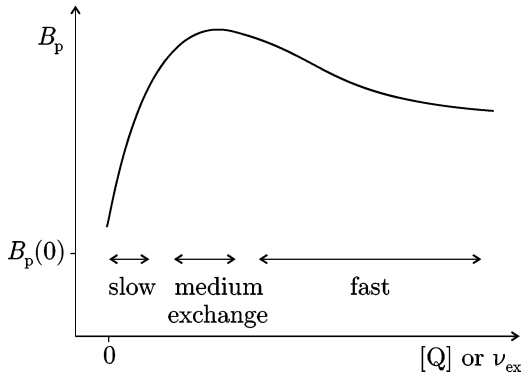

Figure 3. Schematic representation of the dependence of B_p on the self-exchange rate ν_{ex} or on the concentration of neutral donor or acceptor. The exchange rate is related to the molecule concentration (Q = D, A) via eq 2.

k. From the average nuclear HF fields of the two radicals, the $B_{1/2}$-value can be estimated according to[26]

$$B_{1/2} = \frac{2(B_1^2 + B_2^2)}{B_1 + B_2} \tag{7}$$

This formula approximately reproduces the $B_{1/2}$-values found experimentally.[20]

The situation gets more complicated if electron self-exchange adds to the MARY process. The shortening of the electron residence time τ of a given nuclear spin configuration perturbs the coherent spin evolution in the RP and hence changes the singlet recombination yield. The consequence is an influence on the MARY spectrum, in particular with respect to the line width, as has been shown both theoretically[27,28] and experimentally.[14−17,20−22,29,30] The line width behavior with increasing self-exchange rate is illustrated schematically in Figure 3.

The initial increase in the line width may be explained by energy broadening of the RP spin levels due to Heisenberg's uncertainty principle according to

$$\Delta E \geq \frac{\hbar}{\tau} \tag{8}$$

which allows one to express the line width parameter $B_{1/2}$ as a function of [Q] as[14]

$$B_{1/2}([Q]) \approx B_{1/2}(0) + \frac{\hbar}{g_e \mu_B} k_{ex}[Q] \tag{9}$$

where g_e and μ_B are the *g*-factor of the free electron and the Bohr magneton, respectively. Equation 9 may be used for a rough estimation of k_{ex} in the limit of slow exchange.[20−22] When going to intermediate and fast exchange rates, a different effect opposing the line broadening occurs. The reduced nuclear spin configuration lifetime has the effect of weakening the HF coupling of the radical undergoing the exchange, resulting in a decrease in the line width.[16,22] At very fast exchange rates, the effective HF coupling in the RP is determined by that of the nonexchanging radical only, which explains the saturation tendency. The behavior of the line width as shown in Figure 3 is thus characterized by the competition between energy level broadening and averaging of the HF interactions of the exchanging radical. The larger the HF coupling of the radical, the higher the S−T mixing frequency, and the shorter the time required for sufficient spin mixing. As a consequence, if the exchanging radical has a larger B_k, the maximum in a plot like Figure 3 is expected to occur at larger exchange rates ν_{ex}.

3.2. Calculation of Exchange-Affected MARY Spectra. Although the effect of degenerate electron exchange on the magnetic-field-affected singlet and triplet recombination yield of radical pairs has been treated theoretically in the literature,[11,16,17,27,28,31−37] both in a semiclassical and in a quantum mechanical way, no rigorous quantum mechanical calculations of exchange-affected MARY spectra of RP systems containing more than two different HF coupling constants have been so far presented. In the following we present the ab initio calculation of MARY spectra of the systems investigated experimentally, taking into account electron self-exchange over the whole range of exchange rates. On one hand, these simulations serve to gain a deeper understanding of the way parameters such as the radicals' HF coupling constants, the self-exchange rate, or RP recombination kinetics affect the line width and the shape of the MARY spectra, including the low-field feature. On the other hand, the comparison of line widths of the simulated spectra with those of the experimental spectra provides a consistent and reliable method to determine self-exchange rate constants by MARY spectroscopy. It is thus possible to check the validity of the slow exchange limit approach used in previous work.[20−22]

The MARY spectrum is directly related to the product yield ϕ_B of the luminescent species at a given magnetic field *B*, as expressed in eq 4. The reaction scheme of the MARY process (Figure 1) shows that the luminescent species, the exciplex, constitutes a singlet recombination product of the RP. Hence the fluorescence intensity is a function of the singlet recombination yield $\phi_S(B)$ (cf. eq 4 with $\phi_B \equiv \phi_S(B)$). Any magnetic-field-independent contribution to the fluorescence intensity influences only the intensity of the MARY spectrum via a constant scaling factor without changing the spectral shape or the line width.

Consequently, the quantity of key interest for the calculation of MARY spectra is the RP singlet recombination yield $\phi_S(B)$, called singlet yield henceforth. The singlet yield basically depends on two factors: the probability $f(t)$ that the radicals first encounter one another at time *t* and the probability $p_S(B, t)$ of finding the RP in the singlet state at the same instant. Assuming that the radical pairs undergo free Brownian motion,

(27) Schulten, K.; Wolynes, P. J. *J. Chem. Phys.* **1978**, *68* (7), 3292.
(28) Knapp, E.-W.; Schulten, K. *J. Chem. Phys.* **1979**, *71* (4), 1878.
(29) Sviridenko, F. B.; Stass, D. V.; Molin, Y. N. *Chem. Phys. Lett.* **1998**, *297*, 343.
(30) Petrov, N. K.; Alfimov, M. V.; Budyka, M. F.; Gavrishova, T. N.; Staerk, H. *J. Chem. Phys. A* **1999**, *103*, 9601.
(31) Werner, H. J.; Schulten, Z.; Schulten, K. *J. Chem. Phys.* **1977**, *67*, 646.
(32) Stass, D. V.; Lukzen, N. N.; Tadjikov, B. M.; Grigoryantz, V. M.; Molin, Y. N. *Chem. Phys. Lett.* **1995**, *243*, 533.
(33) Gorelik, V. R.; Bagryanskaya, E. G.; Lukzen, N. N.; Koptyug, I. V.; Perov, V. V.; Sagdeev, R. Z. *J. Phys. Chem.* **1996**, *100*, 5800.
(34) Leshina, T. V.; Kruppa, A. I.; Sagdeev, R. Z.; Salikhov, K. M.; Sarvarov, F. V. *Chem. Phys.* **1982**, *67*, 27.
(35) Bagryanskaya, E. G.; Avdievich, N. I.; Grishin, Y. A.; Sagdeev, R. Z. *Chem. Phys.* **1989**, *135*, 123.
(36) Bagryanskaya, E. G.; Sagdeev, R. Z. *Prog. React. Kinet.* **1993**, *18*, 63.
(37) Burri, J.; Fischer, H. *Chem. Phys.* **1992**, *161*, 429.

the singlet yield is given approximately by the integral[28,38]

$$\phi_S(B) = \int_0^\infty p_S(B, t)\, f(t)\, dt \tag{10}$$

Radical pair recombination is treated within a diffusion model based on Noyes' random flight model[39,40] which proved more satisfactory than the simpler exponential model.[23,39] The recombination function is given by

$$f(t) = at^{-3/2} \exp(-b/t) \tag{11}$$

with

$$a = \frac{r_\sigma(r_0 - r_\sigma)}{r_0\sqrt{4\pi D}} \tag{12}$$

and

$$b = \frac{(r_0 - r_\sigma)^2}{4D} \tag{13}$$

where D is the relative diffusion coefficient. The radicals forming the pair are assumed to be created at the separation distance r_0. If they approach to the recombination distance r_σ, recombination occurs with probability 1 if the RP is in its singlet state while triplet encounters are unreactive. Equation 11 thus describes the time distribution of first encounters, ignoring reencounters. This corresponds to the so-called "low viscosity approximation"[41,42] which is applicable if $\omega\tau_D \ll 1$. Here ω is a rough measure of the relevant magnetic field strengths (HF couplings and external magnetic field), and τ_D is the diffusional lifetime defined as

$$\tau_D = \frac{r_\sigma^{\,2}}{D} \tag{14}$$

The influence of D as well as of the radii r_0 and r_σ on the shape of $\phi_S(B)$ is found to be negligibly small, both in the literature[28,31] and in the present work.[23] This fact may be rationalized as follows. It is very reasonable to assume that the radicals of the radical ion pair are formed at a distance close to contact. Thus the values of b in eq 11 may change as a function of D, r_0, and r_σ, but they are definitely much smaller for the given, low viscosities than $1/\omega$, the order of time in which spin dynamics develops. The contribution of this time interval (in the order of b) to the MARY spectra is thus nonmagnetosensitive and is therefore negligible. Thus, for all simulations of MARY spectra, the following parameters are used without exception: $r_0 = 9.0$ Å, $r_\sigma = 5.0$ Å, and $D = 1.0 \times 10^{-5}$ cm^2 s^{-1}, giving rise to a diffusional lifetime of $\tau_D = 0.25$ ns.

The time evolution of the singlet probability $p_S(B, t)$ is governed both by the magnetic interactions experienced by the spins of the unpaired electrons (hyperfine and Zeeman interactions) and by the degenerate electron exchange process. Since the average exchange interaction J between the unpaired electrons of nonlinked radicals is negligibly small, J is assumed to be zero. The parameters entering the calculation of $p_S(B, t)$ are hence a_{ik}, B, and τ.

Besides affecting spin motion, the degenerate electron exchange may change the spatial position of the radical. Under the usual experimental conditions (temperature, pressure), the electron transfer can be considered as a contact reaction. To be accurate, one has to consider the stochastic motion the radical ion which undergoes the self-exchange as continuous diffusion being from time to time interrupted by jumps of the length of the double radius of the radical ion and in a stochastic direction. Although in principle such a problem can be solved, it appears that such an effect is significant only at low viscosities and for large molecules. In fact, one can safely neglect this effect if the displacement of the radical due to continuous diffusion during the time interval between two electron self-exchange events is larger than the jump distance $2R$, where R is the radius of the radical, i.e., $\sqrt{D\tau} \geq 2R$. The criterium is thus $\tau \geq 4R^2/D$. For $R = 5$ Å and $D = 1.0 \times 10^{-5}$ cm^2 s^{-1}, we have $\tau \geq 1$ ns which is generally true of the systems considered.

The procedure to calculate $p_S(B, t)$ is based on the idea of treating the electron spin evolution of each radical of the pair *separately* in terms of so-called spin correlation tensors (SCTs).[27,28,32,43−45] This is possible due to the assumption of zero exchange interaction. The concept was developed by Schulten and co-workers[27,28] in their semiclassical treatment of the spin evolution of RPs in external magnetic fields. In the present work, however, exact quantum mechanical calculations replace the semiclassical approximation accounting for the magnetic interactions, allowing the rigorous quantum mechanical calculation of *real spin systems*.

The time evolution of the electron spin operators $\mathbf{S}_1(t)$ and $\mathbf{S}_2(t)$ of each separate radical 1 and 2 under the HF interaction and the external magnetic field is calculated in a quantum mechanical way, yielding the spin correlation tensors $T^1(t)$ and $T^2(t)$. The SCT of radical 2 is modified to account for the effect of electron self-exchange in a way derived from a separate radical treatment outlined in ref 33. Finally, $T^1(t)$ and $T^2(t)$ are coupled to yield the singlet probability $p_S(B, t)$ of the RP. There are three factors that, taken together, make the calculation of real RP systems possible: (1) circumventing the treatment of the large spin system of the whole RP by calculating the two smaller systems of the individual radicals leads to considerably smaller dimensions of the matrices involved; (2) the calculations are carried out in Hilbert space; i.e., one avoids switching to Liouville space which would be necessary in a density matrix treatment of the complete RP, involving huge matrix dimensions; (3) the existence of groups of equivalent nuclei in the experimental systems (e.g. pyrene/DCB isomers) opens a third possibility to keep matrix dimensions relatively low.

All calculations are carried out in the product spin basis, the first position in the representation ($\langle\alpha\alpha\cdots\alpha\alpha|$, $\langle\alpha\alpha\cdots\alpha\beta|$, etc.) referring to the electron, while all the others refer to the

(38) Steiner, U. E.; Ulrich, T. *Chem. Rev.* **1989**, *89*, 51.
(39) Salikhov, K. M.; Molin, Y. N.; Sagdeev, R. Z.; Buchachenko, A. L. *Spin Polarization and Magnetic Effects in Radical Reactions*, Vol. 22 of *Studies in Physical and Theoretical Chemistry*; Elsevier: Amsterdam, 1984.
(40) Noyes, R. M. *J. Chem. Phys.* **1954**, *22*, 1349.
(41) Osintsev, A. M.; Purtov, P. A.; Salikhov, K. M. *Chem. Phys.* **1993**, *174*, 237.
(42) Purtov, P. A.; Doktorov, A. B. *Chem. Phys.* **1993**, *178*, 47.
(43) Lukzen, N. N.; Usov, O. M.; Molin, Y. N. *Phys. Chem. Chem. Phys.* **2002**, *4*, 5249.
(44) Bagryansky, V. A.; Borovkov, V. I.; Molin, Y. N. *Mol. Phys.* **2002**, *100*, 1071.
(45) Anishchik, S. V.; Borovkov, V. I.; Ivannikov, V. I.; Shebolaev, I. V.; Chernousov, Y. D.; Lukzen, N. N.; Anisimov, O. A.; Molin, Y. N. *Chem. Phys.* **1999**, *242*, 319.

coupled nuclei of the radical. The spin Hamiltonian of radical k is given by

$$H_k = \omega_0 S_z^k + \sum_i a_{ik} \mathbf{S}_k \cdot \mathbf{I}_{ik} \quad (15)$$

where ω_0 is the external field strength expressed in angular frequency units, S_z^k, $\mathbf{S}_k$, and $\mathbf{I}_{ik}$ are the respective electron and nuclear spin operators, and i denotes the nucleus coupling to the electron. For a radical containing groups of equivalent nuclei (like pyrene and the DCB radicals), a number of simpler Hamiltonians replace expression 15 as shown in the following for the case of 1,4-DCB. The 1,4-DCB radical cation contains four equivalent protons with HF coupling constant a_H and two equivalent nitrogens with HF coupling constant a_N. The individual spins of an ensemble of equivalent nuclei can sum up to different total spins $\vec{F}^{H(N)}$ with spin quantum numbers $F^{H(N)}$ according to the vector sums

$$\vec{F}^H = \vec{I}_1{}^H + \vec{I}_2{}^H + \vec{I}_3{}^H + \vec{I}_4{}^H$$
$$\vec{F}^N = \vec{I}_1{}^N + \vec{I}_2{}^N \quad (16)$$

where $\vec{I}_i{}^{H(N)}$ are the spins of individual nuclei i. For instance, the four protons can sum up to yield $F^H = 2$, 1, or 0 in one, three, and two different ways, respectively. The two nitrogens can sum up to $F^N = 2$, 1, 0 in one single way each. The numbers n_{ik} of ways to realize a given total spin are derived from the line intensity pattern of the hypothetical EPR stick spectrum of the ensemble. For the example of four equivalent protons, the EPR line intensity pattern is 1:4:6:4:1. This pattern can be thought of arising from 1 spin−2 nuclei, 3 spin−1 nucleus, and 2 spin−0 nucleus, hence $n_{ik} = 1$, 3, and 2. The corresponding spin operators $\mathbf{F}^{H(N)}$ are calculated using the scheme given in the appendix of ref 46.

For each combination of total spins F^H and F^N, a Hamiltonian is calculated according to

$$H^i_{1,4-DCB} = \omega_0 S_z + a_H \mathbf{S}\cdot\mathbf{F}^H + a_N \mathbf{S}\cdot\mathbf{F}^N \quad (17)$$

with i denoting the nuclear spin configuration of which there are $3 \times 3 = 9$ for 1,4-DCB. The same procedure is done for the pyrene radical cation whose groups of equivalent magnetic nuclei are 4, 4, and 2 H, leading to 18 different Hamiltonians. Now, for all these spin configurations, the time-dependent SCTs for the two radicals can be calculated. Each SCT is represented by a 3×3 matrix, the 3 dimensions accounting for the x-, y-, and z-coordinates. The matrix elements are defined according to

$$T^{ik}_{uv}(t) = \mathrm{Tr}(S^{ik}_u(t) S^{ik}_v(0)) \; (u, v = x, y, z) \quad (18)$$

where $T^{ik}_{uv}(t)$ refers to the ith nuclear spin configuration of radical k and the operators $S^{ik}_u(t)$ and $S^{ik}_v(t)$ are defined in the full nuclear-electron product spin basis of configuration ik. The time evolution of the electron spin operator of configuration ik is given by

$$\mathbf{S}_{ik}(t) = \exp(iH_{ik}t)\mathbf{S}_{ik}(0)\exp(-iH_{ik}t) \quad (19)$$

The total SCT of radical k is given by the weighted sum of the contributions $T_{ik}(t)$,

$$T^k_0(t) = f_k \sum_i n_{ik} T^{ik}(t) \quad (20)$$

with n_{ik} being the number of ways of realizing spin configuration i in radical k (see above) and f_k being a normalization factor accounting for the spin dimension of radical k according to

$$f_k = \frac{4}{\sum_i n_{ik} m_{ik}} \quad (21)$$

with m_{ik} being the dimension (nuclei plus electron) of spin configuration ik. The normalization causes $T^k_0(t)$ to equal the unit matrix at $t = 0$. The subscript 0 in eq 20 denotes that no electron self-exchange takes place. The electron self-exchange of one RP partner is accounted for by a modulation of the respective SCT according to[23,33]

$$T^k(t) = T^k_0(t)\exp\left(-\frac{t}{\tau}\right) + \frac{1}{\tau}\int_0^t T^k_0(t-\xi)\exp\left(-\frac{t-\xi}{\tau}\right)T^k(\xi)\,d\xi \quad (22)$$

where τ is the nuclear spin configuration lifetime. A proof of eq 22 and the procedure for its numerical solution are given in the appendix. Finally, the singlet probability is given by[45]

$$p_S(t) = \frac{1}{4} + \frac{1}{4}\sum_{u,v=x,y,z} T_{uv}{}^1(t)\, T_{uv}{}^2(t) \quad (23)$$

The singlet yield $\phi_S(B)$ is obtained by numerical integration of eq 10. The time range for which all calculations are done is 0 to 1000 ns with time step $\Delta t = 1$ ns. The recombination function $f(t)$ is multiplied by an additional factor $\exp(-t/\tau_{rel})$ accounting for spin relaxation. The spin relaxation time ($\tau_{rel} = T_1 = T_2$ where T_1 and T_2 are the longitudinal and transversal spin relaxation times, respectively) is set to the realistic value of 200 ns in all simulations. This term has the effect of causing $f(t)$ to decay more rapidly, thus providing a good justification for the finite upper integration limit used in the calculations. Increasing $T_1(= T_2)$ from 200 ns to larger values has no visible effect on the MARY spectra. Moreover, the decay of the $t^{-3/2}$-function on the integration interval (1000 ns) provides good convergence of integral 10 even without such apodization.

4. Results and Discussion

4.1. Simulations: from the two-proton RP to a Real System. In this section, the improvements obtained by including increasing numbers of nuclei in the simulation of MARY spectra will be demonstrated using pyrene/1,4-DCB as an example. Simulations are presented for the simple two-proton model RP, for the more realistic four-proton-one-nitrogen model RP as well as for the all-nuclei RP.

In the model RP systems, artificial, effective HF coupling constants are attributed to the model nuclei. A group of (not necessarily equivalent) real nuclei with HF coupling constants a_i and spins I_i is replaced by a single model nucleus of spin $^1/_2$ or spin 1 with an effective coupling constant a_{eff}. Its value is obtained by applying the semiclassical root-mean-square formula for B_k (eq 6) to the group of nuclei to be replaced by the model

(46) Weil, J. A.; Bolton, J. R.; Wertz, J. E. *Electron Paramagnetic Resonance*; John Wiley and Sons: New York, 1994.

Table 1. Model RP Systems for Which Simulations Are Done and Effective HF Coupling Constants a_{eff} Calculated According to Equation 24, Using the HF Coupling Constants from Table 2

RP system	simulated as	a_{eff} (mT)
pyrene/1,4-DCB	3H:1H1N	pyrene: 1.08 (H); 0.42 (H); 0.17 (H) 1,4-DCB: 0.32 (H); 0.26 (N)
	1H:1H	pyrene: 1.17 (H) 1,4-DCB: 0.53 (H)
pyrene-d_{10}/1,4-DCB	3D:1H1N	pyrene: 0.16 (D), 0.07 (D), 0.03 (D) 1,4-DCB: 0.32 (H); 0.26 (N)
MCBZ/1,2-DCB	4H1N:1H1N	MCBZ: 0.47 (H); 0.35 (H); 0.26 (H); 1.64 (H); 0.82 (N) 1,2-DCB: 0.59 (H); 0.25 (N)
MCBZ/1,4-DCB	4H1N:1H1N	MCBZ: 0.47 (H); 0.35 (H); 0.26 (H); 1.64 (H); 0.82 (N) 1,4-DCB: 0.32 (H); 0.26 (N)

Table 2. HF Coupling Constants of the Radicals Investigated

radical	a (mT)	ref
pyrene$^{\bullet+}$	0.547 (4 H); 0.212 (4 H); 0.118 (2 H)	47
pyrene-$d_{10}^{\bullet+}$ [a]	0.083 (4 D); 0.033 (4 D); 0.018 (2 D)	
MCBZ$^{\bullet+}$	0.330 (2 H); 0.083 (2 H); 0.250 (2 H) 0.165 (2 H); 0.946 (3 H, CH_3); 0.82 (N)	48
1,2-DCB$^{\bullet-}$	0.415 (2 H); 0.042 (2 H); 0.177 (2 N)	49
1,4-DCB$^{\bullet-}$	0.159 (4 H); 0.181 (2 N)	49

[a] The values for pyrene-d_{10} are calculated from the pyrene coupling constants using eq 25.

nucleus. Since the value of B_k should be the same before and after the replacement, a_{eff} is given by

$$a_{eff} = \sqrt{\frac{1}{I_m(I_m+1)}\sum_i a_i^2 I_i(I_i+1)} \qquad (24)$$

where I_m is the spin of the model nucleus. The values of a_{eff} for the model RP systems discussed here and in the following sections are given in Table 1. The notation used to specify the model RPs follows the scheme "nuclei of nonexchanging radical:nuclei of exchanging radical".

The HF coupling constants of the radicals studied are given in Table 2. Since no literature values for the deuterium HF coupling constants of pyrene-d_{10} have been found, their values are estimated from the corresponding proton couplings using the ratio

$$\frac{a_D}{a_H} \approx \frac{g_{n,D}}{g_{n,H}} = \frac{0.857}{5.586} \cong 0.15 \qquad (25)$$

where $g_{n,H}$ and $g_{n,D}$ are the respective nuclear g-factors (values are taken from ref 46).

MARY spectra simulated for pyrene/1,4-DCB at two different self-exchange rates are shown in Figure 4, the real system being represented by the 1H:1H RP, the 3H:1H1N RP as well as by the all-nuclei system. The intensities of the spectra are correct except for a scaling factor; therefore no units are given on the ordinate. The simulated spectra, like their experimental counterparts, exhibit in addition to the normal MFE a low-field feature which gets more important for larger values of ν_{ex} (for a detailed discussion see section 4.2).

The increase in the size of the simulated spin system manifests itself in a change in the shape of the low-field feature at very slow exchange ($\nu_{ex} = 5.0 \times 10^6\ s^{-1}$) and in a decrease in the size of the LFE at faster exchange rates ($\nu_{ex} = 1.0 \times 10^9\ s^{-1}$), with the main peak becoming more pronounced. A comparison with experimental spectra (see Figure 6) shows that both findings clearly confirm the expected trend that the quality of the simulations gradually increases with the number of spins included in the model RP. While in the 1H:1H RP, the nitrogens and protons of 1,4-DCB are represented by a single spin-$^1/_2$ model nucleus, in the case of the 3H:1H1N RP we have the more adequate situation that each group of equivalent nuclei in the real pyrene/1,4-DCB system is represented by one model nucleus of the appropriate spin.

The correctness of the numerical procedure of the SCT approach has been additionally confirmed by simulations of the simple model systems using a density matrix approach, calculating the spin evolution of the whole RP rather than of the individual radicals. When applied to the same spin system, both calculation methods give exactly the same result.[23]

For the all-nuclei RP of pyrene/1,4-DCB, the computing time on a Unix Workstation (194 MHz, CPU: MIPS R 10000) is 2600 s per B-point, for 10 different τ-values and 1000 points in time; that is, the calculation of MARY spectra for 10 spin configuration lifetimes with 80 B-points each (on the positive field axis) takes about 60 h.

The behavior of B_p versus the self-exchange rate ν_{ex} for the spectra obtained by simulations of the different spin systems representing pyrene/1,4-DCB is shown in Figure 5. The simulations of all three spin systems qualitatively reproduce the line width behavior found in the experiments. The main differences between the simpler and the more complex spin systems concern the maximum increase in B_p, the extent of decrease after the maximum, and the position of the maximum. The more spins that are included in the simulation, the flatter the curve becomes.

Figure 5 shows clearly that the approximate approaches (1H:1H and 3H:1H1N) are inadequate because of the large differences between them and the exact approach which should therefore be preferred.

4.2. Simulated and Experimental MARY Spectra. The appearance of both the experimental and simulated spectra primarily depends on the HF coupling situation in the RP as well as on the rate of electron self-exchange. The shape of the experimental spectrum is, in addition, influenced by the resolution of the experiment as determined by the modulation amplitude which itself is dictated by the S/N ratio of the system. The S/N ratio is strongly determined by the details of the photochemistry of the system as well as by solvent properties such as viscosity and dielectric constant. It is hard to observe a general correlation between the size of the MFE and the solvent parameters. However, it seems that a minimum dielectric constant ($\epsilon \approx 5$) is required to observe an MFE. This finding can be understood in view of ion pair stabilization by the solvent which must be sufficient to allow the formation of RIPs. An important role is also played by the viscosity which influences the RP lifetime and hence the time available for magnetic field-affected spin mixing.

The broad main peak of the spectrum is not sensitive to the field modulation, the main effect of the modulation technique being to attenuate the low-field feature. Consequently, in many cases not all the features of a calculated spectrum are found in the experimental spectrum to the same degree. The systems pyrene/1,2-DCB and pyrene/1,4-DCB in THF as well as pyrene-

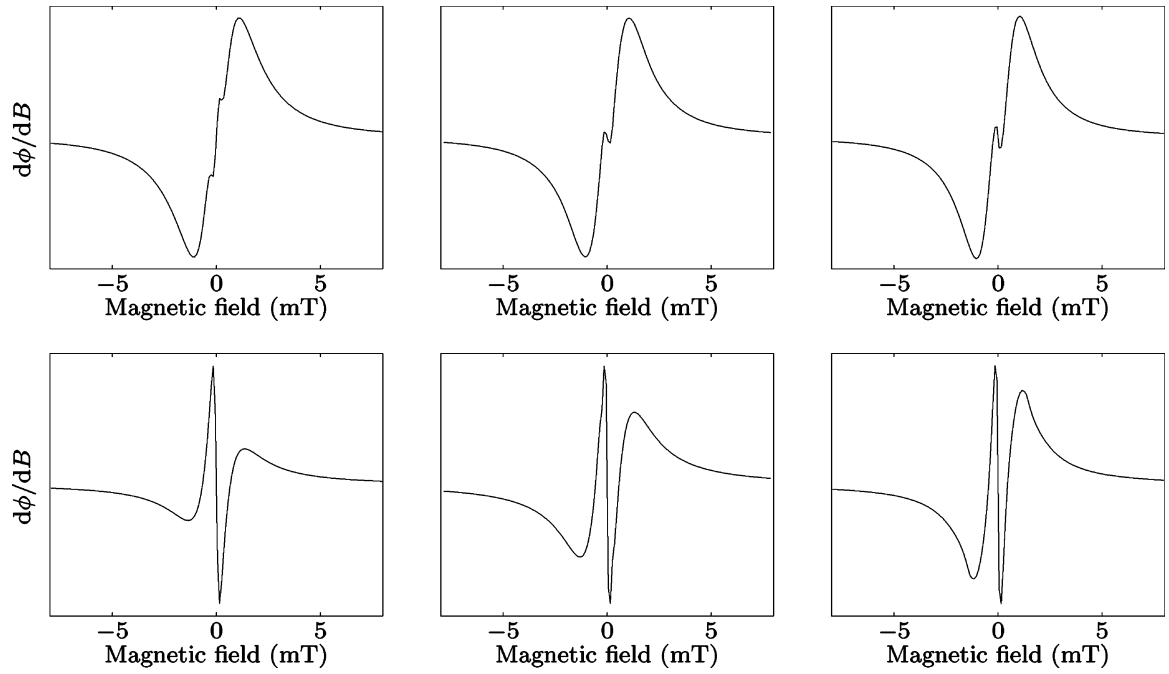

Figure 4. Exchange-affected MARY spectra calculated for the pyrene/1,4-DCB system represented by different spin systems. (Left) 1H:1H RP; (center) 3H:1H1N RP; (right) all-nuclei RP. HF coupling constants are given in Tables 1 and 2. The radical undergoing degenerate electron exchange is 1,4-DCB. (Top) $\nu_{ex} = 5.0 \times 10^6\ s^{-1}$, (bottom) $\nu_{ex} = 1.0 \times 10^9\ s^{-1}$.

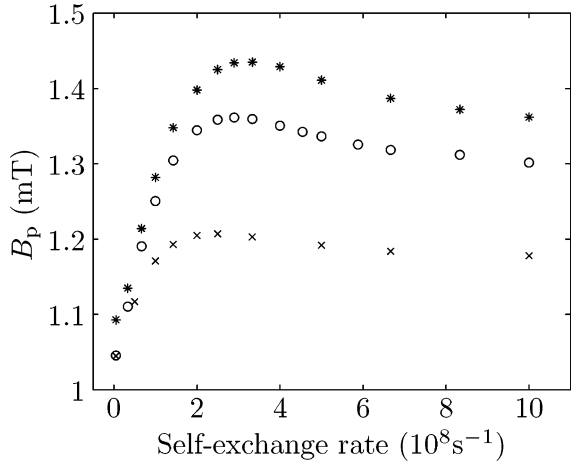

Figure 5. Line width behavior B_p vs self-exchange rate of MARY spectra calculated for the pyrene/1,4-DCB system using different methods. (*) 1H:1H RP; (○) 3H:1H1N RP; (×) all-nuclei RP (HF coupling constants are the same as in Figure 4). The B_p-values are determined from the zero-crossing of the second derivative of the simulated MARY spectra.

d_{10}/1,4-DCB in THF serve to illustrate the degree of agreement between experiment and simulation. For both of these systems, MARY spectra recorded at three different DCB concentrations are compared to the simulations performed for corresponding self-exchange rates ν_{ex}.

For the systems pyrene/1,2-DCB and pyrene /1,4-DCB in THF shown in Figure 6, experimental as well as simulated spectra exhibit a low-field feature which increases with the molecular concentration (self-exchange rate) of the respective RP partner. This behavior can be interpreted in view of the fact that the LFE is particularly large if one of the radicals has no HF couplings at all.[25] The effect of a decreasing τ is to cause a "weakening" of the HF coupling of the exchanging radical, eventually leading to a situation that comes close to that in the absence of HF coupling. It is hence the "removal" of the HF coupling of the exchanging radical that is responsible for the growing LFE with the increasing exchange rate.

The perdeuterated derivative pyrene-d_{10}, although having the same number of couplings with the same grouping into sets of equivalent nuclei as pyrene itself, poses significantly higher demands concerning computational resources for its calculation. The replacement of the 10 hydrogens with $I = {}^1/_2$ by deuteriums with $I = 1$ causes a significant increase in both the spin dimensions and the number of spin configurations to be averaged in the calculations. Therefore, the simpler 3D:1H1N RP with the HF constants given in Table 1 is chosen as a model system for simulations. There are two striking differences in the MARY spectra of pyrene-d_{10}/1,4-DCB shown in Figure 7 as compared to the protonated analogue: first, the much smaller line width B_p which is hardly surprising in view of the smaller HF couplings and, second, the absence of the low-field feature. Both experimental observations are excellently reproduced by the simulations. Only at the highest self-exchange frequency ν_{ex} does a very narrow low-field feature appear in the simulation; the width of this feature is way below the resolution of the experiment. Bearing in mind that the observed MARY spectrum results from the superposition of low-field effect and normal MFE, the reason for the absence of the phase-inverted peak around zero field may be its coincidence with the narrow main peak.

4.3. Determination of Electron Self-Exchange Rate Constants. The discussion is now focused on the concentration dependence of the line width which is the basis for the investigation of self-exchange kinetics. As stated earlier, with increasing concentration of one of the RP partner, the line width first increases, reaches a maximum, and then eventually decreases again to reach a saturation value. Due to practical constraints such as limited solubility of the exchanging species, for some RP−solvent combinations only the initial broadening

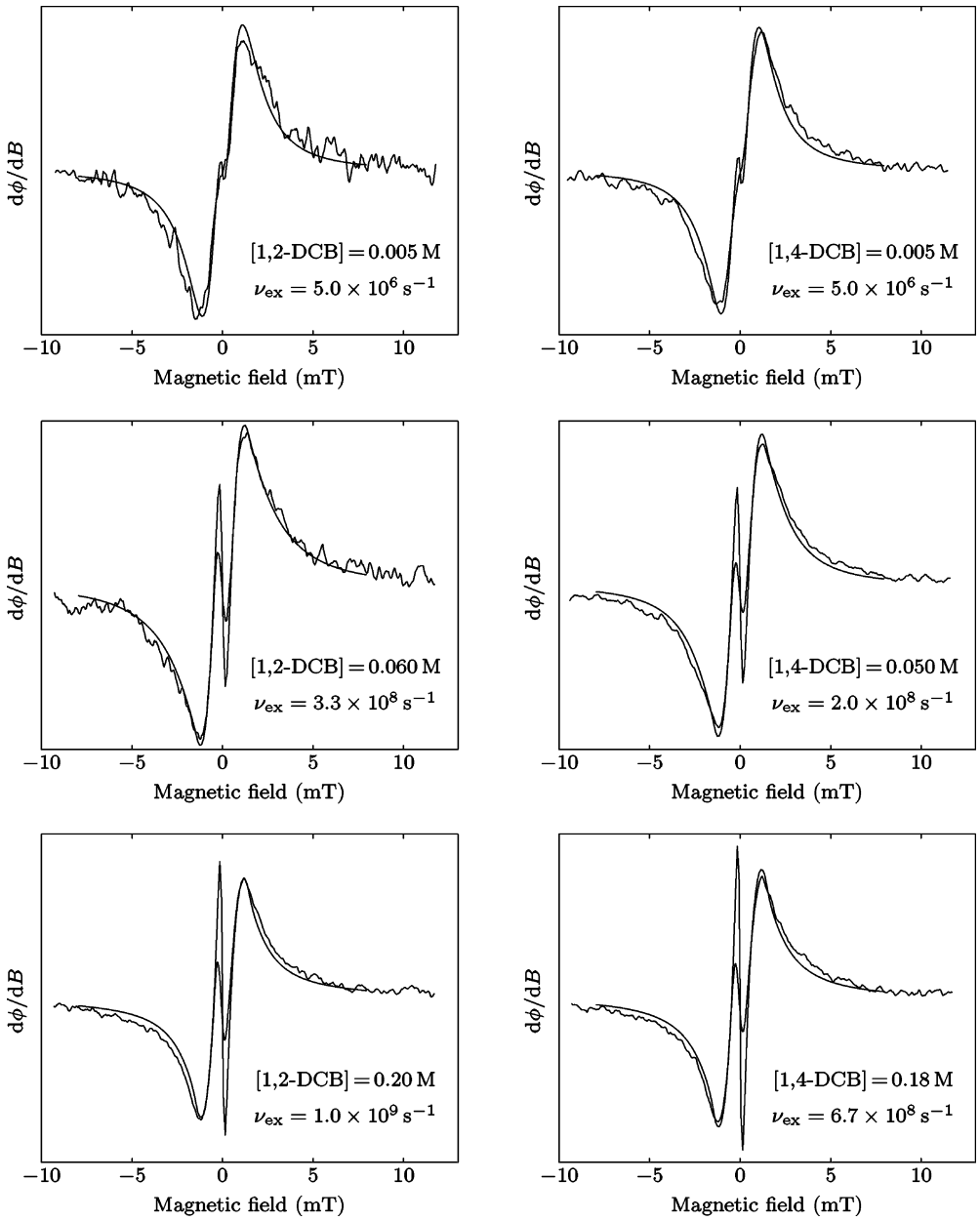

Figure 6. Experimental MARY spectra of pyrene/1,2-DCB in THF (left) and pyrene/1,4-DCB in THF (right) and corresponding all-nuclei simulations (smooth lines). Experiment (noisy lines): [pyrene] = 1.0×10^{-4} M, B_{mod} = 0.2 mT. The self-exchange rate (i.e., [DCB] in the experiment) increases from top to bottom. In all cases, the simulated spectra show a larger low-field feature than the experimental spectra.

corresponding to the slow to medium exchange region in the B_p vs concentration curve can be observed experimentally.

The line width behavior of experimental and simulated MARY spectra for the systems pyrene/1,2-DCB and pyrene/1,4-DCB in THF with respect to the DCB concentration is shown in Figure 8. For the sake of comparability, the line widths of both experimental and simulated spectra are determined by the Lorentz fitting procedure described in section 2. Leaving aside the offset, the simulations very well reproduce the experimental results. The larger values of B_p of the experimental spectra may be due to the HF coupling of ^{13}C-nuclei which is not taken into account in the simulations. A possible line width contribution from the small extent of self-exchange of the RP partner kept at constant low concentration (pyrene) can safely be neglected for concentrations $<10^{-3}$M. Assuming a B_p vs concentration plot similar to that of Figure 8, a glance at the figure shows that B_p for a concentration of 10^{-3} M is indistinguishable from the value at concentration zero.

The electron self-exchange rate constant k_{ex} is obtained by matching the curves of experimental and simulated B_p-values using a two-step fitting procedure. First, the functional behavior of experimental B_p vs concentration as well as the behavior of simulated B_p vs ν_{ex} are each fitted by a separate analytical biexponential function. This allows matching the B_p-curves with respect to the *x*-axis in a second fitting step. Since the two B_p-curves have different quantities on their *x*-axes (concentration for the experiment, ν_{ex} for the simulation), the exchange rate ν_{ex} in the B_p-plot of the simulation is replaced by the term *kc*, where *c* is the molecular concentration of the exchanging species. Leaving the parameters of the fitting functions obtained in the first step unaltered, *k* is now fitted with respect to the minimum difference between the *first derivatives* of the

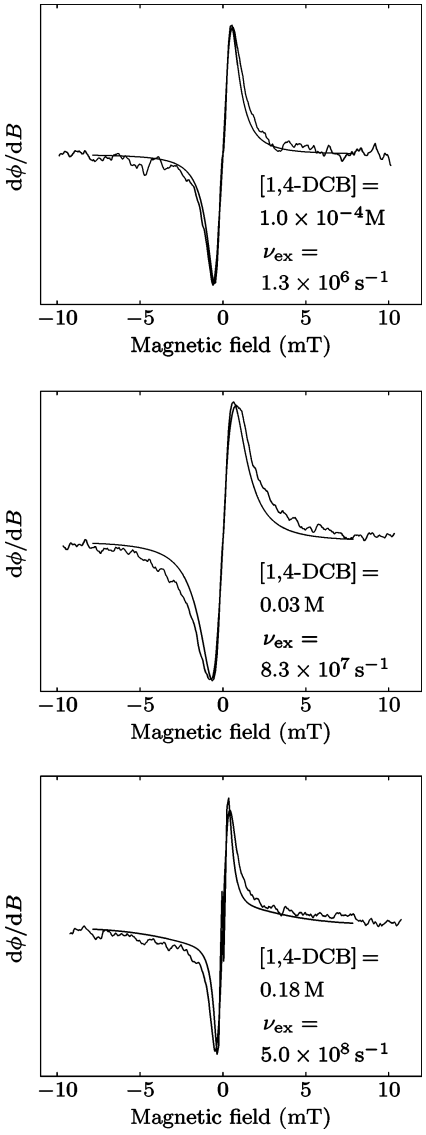

Figure 7. Experimental MARY spectra of pyrene-d_{10}/1,4-DCB in THF (B_{mod} = 0.2 mT) and corresponding simulations as 3D:1H1N RP (HF couplings are given in Table 1). The concentration of pyrene-d_{10} is constant at 1.0 × 10^{-4} M while the 1,4-DCB concentration increases from top to bottom.

biexponential fitting curves of experimental and simulated B_p (see Figure 8). Thus the influence of the offset in B_p is eliminated. The value of k obtained by this fit is taken as k_{ex}.

The line width behavior with respect to the electron self-exchange rate of 1,4-DCB for the system pyrene-d_{10}/1,4-DCB is depicted in Figure 9. As in the MARY spectra themselves, there are pronounced differences in comparison to the system with protonated pyrene. The maximum is more pronounced and occurs at a lower concentration (self-exchange rate) than in the case of pyrene. In particular, the decrease in B_p after the maximum is much more important, with B_p decreasing even below the initial value at slow exchange. This strong decrease in the fast exchange limit can be easily understood in view of the "weakening" of the HF coupling of the exchanging DCB mentioned earlier. In this exchange regime, the only magnetic interactions determining the MARY line width are the small HF couplings of the nonexchanging pyrene-d_{10} radical. The general reason for the more pronounced line width effects lies in the small HF couplings of pyrene-d_{10}, causing B_p to be mainly

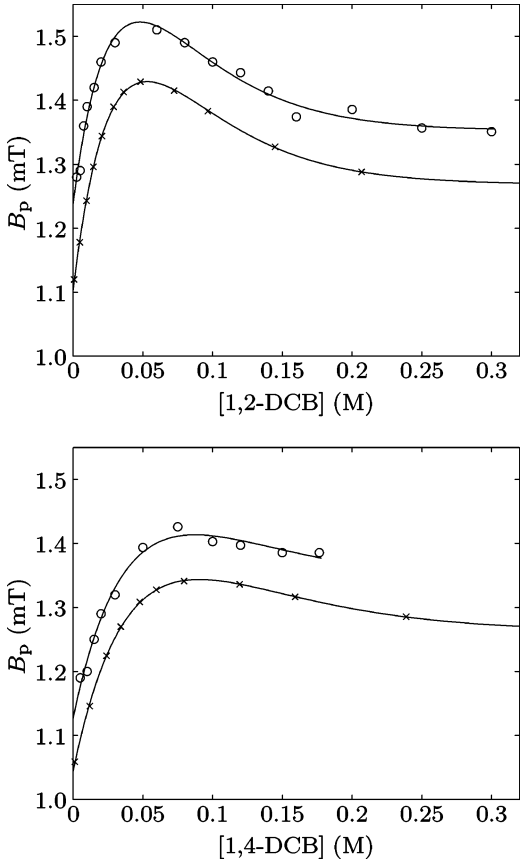

Figure 8. Line width behavior B_p vs concentration of experimental (○, B_{mod} = 0.5 mT) and simulated (×, all-nuclei simulation) MARY spectra of pyrene/1,2-DCB (top) and pyrene/1,4-DCB (bottom) in THF. The lines are biexponential fits of the B_p curves.

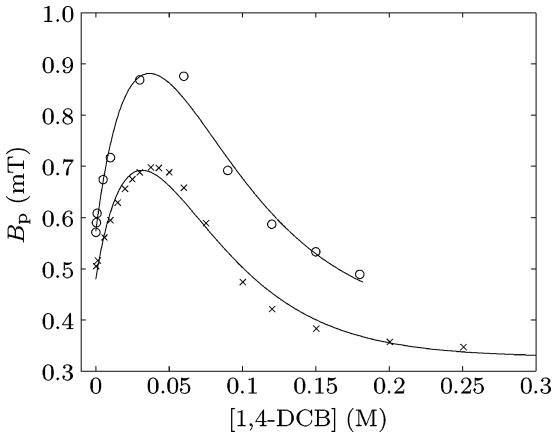

Figure 9. Line width behavior B_p vs concentration of experimental (○, B_{mod} = 0.2 mT) and simulated (×, 3D:1H1N RP) MARY spectra of pyrene-d_{10}/1,4-DCB in THF. The lines are biexponential fits of the B_p curves.

determined by the exchanging 1,4-DCB. Thus the effect of exchange manifests itself more strongly than it can do in the presence of a nonexchanging RP partner with dominant HF couplings.

The simulation method described above may be used to check the simpler initial slope method (eq 9) used in previous work.[20−22] The rate constants for the systems analyzed by the simulation and the initial slope methods are summarized in Table 3. The k_{ex}-values are given together with the modulation amplitude used which was kept as low as possible but large enough to ensure a sufficient S/N ratio of the spectra.

Table 3. Rate Constants k_{ex} of Electron Self-Exchange of R_2 Determined by MARY Spectroscopy Using the Method of Initial Slope (Equation 9) and the Simulation Method, Respectively[a]

R_1	R_2	solvent	B_{mod} (mT)	k_{ex} (10^9 M^{-1} s^{-1}) simulation	k_{ex} (10^9 M^{-1} s^{-1}) initial slope
pyrene	1,2-DCB	THF	0.5	6.9	3
pyrene	1,2-DCB	MeOH	1.0	2.7	1
pyrene	1,2-DCB	PC	1.0	0.64	0.4
pyrene	1,2-DCB	DMF	1.0	1.3	1
pyrene	1,4-DCB	THF	0.5	4.2	2
pyrene	1,4-DCB	PC	1.0	0.78	0.5
pyrene	1,4-DCB	DMF	1.0	1.6	2
pyrene	1,4-DCB	DME	0.5	1.8	1
pyrene	1,4-DCB	BN	0.2	1.1	0.9
pyrene-d_{10}	1,4-DCB	THF	0.2	3.3	7
MCBZ	1,2-DCB	THF	0.5	3.4	1
1,2-DCB	MCBZ	THF	0.5	2.3	2
MCBZ	1,4-DCB	THF	0.5	4.8	1
1,4-DCB	MCBZ	THF	0.5	4.5	4

[a] Relative errors are about 20% for the simulation method, while the results of the initial slope method are to be considered merely as estimations.

The relative error of both methods due to experimental scatter is estimated to be about 20%. The initial slope method yields much less reliable results which should be taken as mere estimations as the following discussion shows.

For most of the systems investigated, the two methods give comparable results, the largest differences being found for the system pyrene-d_{10}/1,4-DCB and the MCBZ systems. The reason for these discrepancies is that the initial slope method neglects one important fact: the slope of the $B_{1/2}$ (or B_p) vs concentration plot is determined not only by the exchange rate constant k_{ex} but also by other parameters, namely the HF couplings of both radicals of the pair. The plots of the two systems pyrene/1,4-DCB and pyrene-d_{10}/1,4-DCB (cf. Figures 8 and 9) show strongly differing initial slopes, resulting in rate constants that differ by a factor of 3.5 when evaluated via the slope. Since there is no good physical reason 1,4-DCB should exchange 3.5 times faster when pyrene-d_{10} is the fluorophore than for protonated pyrene, this result is to be considered as an artifact. This problem does not emerge with the simulation method which inherently takes into account the HF couplings of the radicals. The above reasoning also applies to the systems MCBZ/1,2-DCB and MCBZ/1,4-DCB. It has to be mentioned, however, that the simulations for the simplified model systems (see Table 1) used to represent the MCBZ systems reproduce the experimental line width behavior significantly less successfully than for the pyrene systems, leading to less reliable k_{ex}-values.

Another substantial advantage of the simulation method over the initial slope approach is that it uses the entire information of the B_p vs concentration plot over the whole concentration range rather than being limited to the slow exchange region. Thus by avoiding the arbitrary selection of data points included for the linear fit to yield the slope, the rate constants obtained from the simulations should be far more reliable. In contrast, the initial slope method rather has the character of an estimation.

One possibility to check the self-exchange rate constants obtained by the MARY method is to compare them to the values obtained by the well-established EPR line broadening technique (see Table 4). Although such a comparison is not entirely adequate for reasons discussed in the following, it provides some useful orientation. For the solvents DMF and PC, the agreement

Table 4. Comparison of Observed Electron Self-Exchange Rate Constants k_{ex} as Determined by MARY Spectroscopy and by the EPR Line Broadening Technique

compound	solvent	k_{ex} (10^9 M^{-1} s^{-1}) MARY[a]	k_{ex} (10^9 M^{-1} s^{-1}) EPR	EPR ref
1,2-DCB	THF	6.9	0.93	49
1,2-DCB	PC	0.64	0.54	49
1,2-DCB	DMF	1.3	1.2	50
1,4-DCB	THF	4.2	1.2	49
1,4-DCB	PC	0.78	0.56	49
1,4-DCB	DMF	1.6	1.4	50

[a] The MARY values are determined by the simulation method and refer to systems with pyrene as the non-exchanging RP partner

is good to excellent, while the data for THF differ tremendously, for 1,2-DCB by almost an order of magnitude. To explain this apparent discrepancy, one has to be aware of the fact that the two methods, MARY and EPR, investigate *different* self-exchange reactions: in MARY, the underlying electron self-exchange takes place between a neutral molecule and a *radical that is part of a radical pair* (see eq 3), whereas, in the EPR case, the electron is transferred between a neutral molecule and a *free radical* according to eq 1. Therefore one would expect that the MARY rate constants might differ from the corresponding EPR values due to RP interactions which may influence the energetics of the exchange process.

However, RP interactions may not be the only factor affecting the exchange kinetics. In the technique applied in ref 49, the DCB radical anions are generated electrolytically in situ in the EPR cavity which requires a supporting electrolyte (tetrabutylammonium tetrafluoroborate). It is known that solvents of rather low polarity like THF favor the process of ion pairing.[51,52] The formation of an ion pair between the DCB radical anion and a corresponding counterion may be responsible for the comparatively slow self-exchange observed in the EPR experiment. Alternatively, different outer sphere reorganization energies for the exchange reactions between the RP and the molecule on one hand and between the radical and the molecule on the other hand may be the origin for the different rate constants observed.

A third reason for the observed differences may be the absence of a Coulombic force potential in the radical pair recombination model which would manifest itself most strongly in the least polar solvent, i.e., THF. This might be an indication of the failure of the free diffusion model and deserves some future work.

5. Conclusion

The theoretical model developed allows unprecedented simulations of exchange-affected MARY spectra of real RP systems in a quantum mechanically exact way, covering the whole range from slow to fast self-exchange rates. The behavior of the width of the MARY line as a function of self-exchange rate (broadening in the slow exchange regime, narrowing at fast exchange) is documented and analyzed both experimentally and theoretically for various RP systems in different solvents. The

(47) Mäkelä, R.; Oksanen, M.; Vuolle, M. *Acta Chem. Scand. A* **1984**, *38*, 73.
(48) Fujita, H.; Yamauchi, J.; Ohya-Nishiguchi, H. *Nippon Kagaku Kaishi* **1989**, *8*, 1344.
(49) Kattnig, D.; Mladenova, B. Personal communication.
(50) Kowert, B. A.; Marcoux, L.; Bard, A. J. *J. Am. Chem. Soc.* **1972**, *94*, 5538.
(51) Piotrowiak, P.; Miller, J. R. *J. Phys. Chem.* **1993**, *97*, 13052.
(52) Kluge, T.; Knoll, H.; Brede, O. *Z. Phys. Chem.* **1995**, *191*, 59.

ab initio simulations provide a novel, consistent, and reliable method for the determination of self-exchange rate constants by MARY spectroscopy. The simple initial slope method used in earlier work is shown to serve merely as a crude estimation.

We show that ab initio calculations of self-exchange require neither extremely long computation times nor a lot of programming efforts. At the same time they are free from the uncertainties concerning the accounting of spin dynamics which the semiclassical approach, e.g., that developed by Schulten's group,[27,28] suffers from. To know just when the semiclassical approach can be applied would be a worthwhile investigation which, however, is beyond the scope of this work.

The correctness of the rate constants obtained by the MARY technique (simulation method) is proved by a comparison with corresponding data obtained by the well-established EPR line broadening technique. However, such a comparison should not be over-interpreted due to the somewhat different self-exchange reactions that are investigated by the two techniques.

The strong point of the MARY technique is that it allows the investigation of radicals that are extremely short-lived. The radicals are created under mild conditions in a photoinduced electron transfer reaction. The demands on RP lifetime are low; a lifetime of a few nanoseconds is sufficient, while for the classical CW EPR line broadening technique the radical lifetime should be at least 100ms. Even CIDEP (chemically induced dynamic electron polarization) techniques require radical lifetimes greater than 10 μs. Thus, MARY spectroscopy is an interesting alternative to EPR in the study of electron self-exchange kinetics of systems involving short-lived radicals.

A drawback of the MARY method is its dependence on the photochemistry of the system to be investigated. In particular, the requirements for the appearance of magnetic field-affected luminescence have to be fulfilled. Moreover, the solvent has an important influence on the occurrence and on the size of the MFE. The choice of solvents is thus limited to those giving a MARY signal strong enough for an accurate determination of the line width.

Future work will focus on the study of new RP systems (such as the DCB isomers in combination with anthracene or chrysene). The MARY spectra of these systems can readily be calculated within the all-nuclei approach presented in this work. The extension of the all-nuclei calculations to larger spin systems (like pyrene-d_{10} and MCBZ) can be achieved by implementing new, memory-saving algorithms and by using larger, more powerful computers. Also, the discrepancy between the results from EPR and MARY will be studied in more detail in a future project.

Another point that needs further work is the refinement of the model of RP recombination, in particular with respect to the inclusion of Coulombic attraction in the recombination function.

An interesting topic on the experimental side will be the investigation of the temperature dependence of k_{ex} to obtain activation parameters of the self-exchange reaction.

Acknowledgment. Financial support from the INTAS (Project 99-1766) as well as from the VW foundation is gratefully acknowledged. N.N.L. would like to thank the RFBR (Russian Foundation for Basic Researches) for a research grant (Grant Number 02-03-32125).

Supporting Information Available: Appendix (3 pages). This material is available free of charge via the Internet at http://pubs.acs.org.

JA0394784